Dalton Transactions

Accepted Manuscript

ROYAL SOCIETY OF CHEMISTRY

www.rsc.org/dalton

Journal Name

RSCPublishing

ARTICLE

Two Cu-complex directed aluminoborates: from 2D layer to 3D framework

Cite this: DOI: 10.1039/xoxxoooooox

Lin Cheng,[a] Jun-Wei Zhao,[b] and Guo-Yu Yang*[a]

Received ooth January 2012,
Accepted ooth January 2012

DOI: 10.1039/xoxxoooooox

www.rsc.org/

With transition metal complexes as the structure-directing agents, two novel aluminoborates with 2-D layer $[Cu(enMe)_2]_3\{Al_2[B_5O_8(OH)_2]_4\}\cdot H_2O$ (**1**, enMe = 1,2-diaminopropane) and 3-D open-framework $[Cu(en)_2][Al\text{-}B_5O_{10}]$ (**2**, en = ethylenediamine) have been solvothermally made and characterized by elemental analysis, IR spectroscopy, thermogravimetric analysis, UV/Vis spectroscopy, powder and single-crystal X-ray diffraction, respectively. **1** is a 2-D $\{Al[B_5O_8(OH)_2]_2\}^{3-}$ layer constructed by the alternate linkages of AlO_4 groups and $B_5O_8(OH)_2$ clusters. The 2-D layer contains 16-member rings (MRs), showing unique *sql* net topology. In **2**, the AlO_4 groups and B_5O_{10} clusters alternately link together to form 3-D framework, in which the stacking of building layers is different. The copper centres chelated by two amine ligands to form a square planar, which have weak axial interactions to the aluminoborate frameworks.

Introduction

Metal borates are well recognized due to their diverse structures and potential applications in mineralogy, ion exchange and optical fields.[1] From the view point of structure, these materials are attracting increasing attention for the preference of B to adopt three-coordinated BO_3 triangle and four-coordinated BO_4 tetrahedron.[2] The further interlinkage of BO_3 and BO_4 geometries gives rise to a large amount of polyborate anions via corner-sharing of O atoms. On the one hand, these polyanionic clusters can be considered as the secondary building units (SBUs) in the construction of extended structures.[3] For instance, The $[B_5O_6(OH)_4]^-$ cluster can be condensed toge-ther by eliminating through dehydration condensation to form 1-D $[B_5O_7(OH)_2]_n^{n-}$ chains.[4] On the other hand, the oxoboron clusters can integrate the metal ions with different coordination modes to enhance the diversity of the architectures.[5]

Aluminium has long been a focus of research in the synthesis of zeolite materials. Being in the same group as B, Al can exhibit flexible coordination behaviour such as tetrahedral AlO_4 trigonal-bipyramidal or square-pyramidal AlO_5 and octahedral AlO_6.[6] By incorporating Al atoms into borate frameworks, a series of aluminoborates (ABOs) have been reported.[7] In these ABOs, various protonated organic amines, inorganic cations and transition-metal complexes play significantly structure-directing role on the formation of ABO frameworks with novel topologies.

In our previous works, the metal complexes (MCs) as structure-directing agents (SDAs) has been considered to be an effective method to make ABOs,[7g,8] because the MCs have unique configurations and different charges. In general, the transition metal cations, such as Ni^{2+}, Co^{2+}, Mn^{2+}, can form six coordinated MCs with six N atoms of the amines and interact with the framework through H-bonds between the coordinated N atoms of the complex and O/OH atoms of the framework. We followed our synthesis strategy for making novel ABOs by changing the central atoms of CMs into Cu^{II} atoms and made two new Cu-complex directed ABOs, $[Cu(enMe)_2]_3\{Al_2[B_5O_8(OH)_2]_4\}\cdot H_2O$ (**1**, enMe = 1,2-diaminopropane) and $[Cu(en)_2][AlB_5O_{10}]$ (**2**, en = ethylenediamine). **1** displays a 2-D net based on unprecedented linkage mode in ABOs, in which the AlO_4 tetrahedra are 4-connected nodes and $B_5O_8(OH)_2$ clusters are linkers, whereas **2** features a 3-D framework with *cag* topology constructed by the stacking of building layers. The Jahn-Teller character of the d^9 Cu^{2+} cation favours the asymmetric coordination to form square-planar coordination environments. The Cu-complexes interacted with the framework not only via long axial Cu-O interactions, but also with numerous H-bonds. To the best of our knowledge, both **1** and **2** are the first examples where the Cu-complexes are directly linked to the ABO frameworks and act as both SDAs and framework-forming units.

[a]*State Key Laboratory of Structural Chemistry, Fujian Institute of Research on the Structure of Matter, Chinese Academy of Sciences, Fuzhou, Fujian 350002 (China). Fax: (+86) 591-8371-0051; E-mail: ygy@fjirsm.ac.cn*
[b]*Henan Key Laboratory of Polyoxometalate Chemistry, College of Chemistry and Chemical Engineering, Henan University, Kaifeng, Henan 475004 (China)*

† Electronic Supplementary Information (ESI) available: Additional structure pictures, PXRD, IR, TG, UV-vis. CCDC-970024-970025. For ESI and crystallographic data in CIF or other electronic format see DOI: 10.1039 /b000000x/.

Experimental Section

Materials and methods

All analytical grade chemicals employed in this study were commercially available and used without further purification. Elemental analyses (C, H and N) were performed using a German Elementary Vario EL III instrument. The solid-state UV/Vis spectra were measured at room temperature using a PE Lambda 950 UV/Vis spectrophotometer, and a $BaSO_4$ plate was used as a standard (100% reflectance). The absorption (F(R)) data were calculated from reflectance spectra by using the Kubelka–Munk function: $F(R) = (1 - R^2)/2R$, where F(R) is the absorption coefficient and R is the reflectance.[9] The FT-IR spectra (KBr pellet) were recorded on an ABB Bomen MB 102 spectrometer in the range of 4000-400 cm^{-1}. Powder X-ray diffraction (PXRD) patterns were recorded in the angular range of 2θ = 5–60° on a Rigaku DMAX 2500 diffractometer using CuKα radiation (λ = 1.5418 Å). Thermo-gravimetric analyses were carried out on a Mettler TGA/SDTA 851e analyser at a heating rate of 10°C min^{-1} under air atmosphere in the temperature region of 30-1000°C.

Synthesis of $[Cu(enMe)_2]_3\{Al_2[B_5O_8(OH)_2]_4\}\cdot H_2O$ (1).

A mixture of Al(i-PrO)$_3$ (0.186 g, 0.9 mmol), H_3BO_3 (0.372 g, 6 mmol), $Cu(OAc)_2\cdot H_2O$ (0.100 g, 0.5 mmol) and a mixed solvent of 1,2-diaminopropane (1 mL), H_2O (0.5 mL) and pyridine (4 mL) was stirred for half an hour. Then the mixture was sealed in a 30 mL teflon-lined stainless steel autoclave and heated at 180°C for 9 days. Then the closed apparatus was taken out from the oven and cooled to room temperature naturally under ambient condition. The products contained block-like purple crystals of **1**, Cu powder and unknown white amorphous phase. The crystals of **1** were selected by hand, washed by distilled water and then dried in air. The yield of the crystals of **1** is 43% based in $Cu(OAc)_2\cdot H_2O$. Anal. Calc. For **1**: C, 13.75; N, 10.69; H, 4.50; found: C, 13.30; N, 10.42; H, 4.56.

Synthesis of $[Cu(en)_2][AlB_5O_{10}]$ (2)

A mixture of Al(i-PrO)$_3$ (0.204 g, 1 mmol), H_3BO_3 (0.372 g, 6 mmol), $Cu(OAc)_2\cdot H_2O$ (0.199 g, 1 mmol) and a mixed solvent of ethylenediamine (1 mL), H_2O (0.5 mL) and pyridine (3.5 mL) was stirred for half an hour. Then the mixture was sealed in a 30 mL teflon-lined stainless steel autoclave and heated at 180°C for 9 days. Then the autoclave was taken out from the oven and cooled to room temperature naturally under ambient condition. The products contained block-like purple crystals of **2**, Cu powder and unknown white amorphous phase. The crystals of **2** were selected by hand, washed by distilled water and then dried in air. The yield of the crystals of **2** is 29% based in $Cu(OAc)_2\cdot H_2O$. Anal. Calc. For **2**: C, 11.31; N, 13.20; H, 3.80; found: C, 10.91; N, 12.98; H, 3.77.

Single-crystal structure determination

The intensity data sets were collected on a Saturn724 CCD with graphite-monochromated Mo-Kα radiation (λ = 0.71073 Å) in the ω scanning mode at room temperature. All absorption corrections were performed using the multiscan program. The structures were solved by direct methods and refined by full-matrix least squares on F^2 with the SHELXTL-97 package.[10] All the non-hydrogen atoms were refined anisotropically. The H atoms of organic amines and water molecules were geometrically placed and refined using a riding model. The C(2) atom in **1** was disordered over two positions with the occupation factors of 0.5 and 0.5, respectively. The relevant crystallographic data and structure refinement details are listed in Table 1, and the selected bond lengths are listed in Table S1. The purities of the compounds were confirmed by XRD powder diffraction studies (Fig. S1).

Table 1 Crystal data and structure refinements for **1** and **2**.

	1	**2**
Empirical formula	$C_{18}H_{70}Al_2B_{20}Cu_3N_{12}O_{41}$	$C_4H_{16}AlB_5CuN_4O_{10}$
Formula weight	1571.67	424.79
Crystal system	Triclinic	Orthorhombic
Space group	*P*-1	*Pbca*
a, Å	9.603(2)	13.3741(8)
b, Å	18.439(4)	13.7633(7)
c, Å	18.741(3)	16.0355(8)
α, deg	104.736(2)	90
β, deg	93.845(2)	90
γ, deg	104.840(1)	90
V, Å3	3071.1(10)	2951.7(3)
Z	2	8
D_c, g cm^{-3}	1.700	1.912
Absorption coefficient, mm^{-1}	1.169	1.599
T, K	293(2)	293(2)
Limiting indices	$-11 \le h \le 11$ $-21 \le k \le 21$ $-21 \le l \le 21$	$-17 \le h \le 17$ $-14 \le k \le 17$ $-19 \le l \le 20$
No. of reflections collected	20257	23512
No. of independent reflections	10497	3380
Data / restrains / parameters	10497/125/873	3380/0/235
Goodness-of-fit on F^2	1.064	1.058
Final *R* indices [$I>2\sigma(I)$]	$R1$ = 0.0703 $wR2$ = 0.1997	$R1$ = 0.0733 $wR2$ = 0.1633
R indices (all data)	$R1$ = 0.0866 $wR2$ = 0.2194	$R1$ = 0.0799 $wR2$ = 0.1667

Results and Discussion

Synthesis

Solvothermal methods have been successfully utilized to make MC-templated ABOs, such as $[Zn(dien)_2][\{Al(OH)\}\{B_5O_9F\}]$,[8] $[M(dien)_2]\{(B_5O_9)[BO_2(OH)]\}$ (M= Co/Ni/Cd/Zn) and $[M(en)_3][AlB_7O_{12}(OH)_2]\cdot(H_2O)_{0.25}$ (M= Co/Ni),[7g] in which the transition metal cations and organic amines are applied as the starting reaction materials and the MCs are formed in situ. Here, we replace the central atoms with copper under similar conditions, resulting in the formations of **1** and **2**. In the synthesis of microporous materials, the Cu-complexes are rarely used as SDAs[11] because the Cu^{II} cations in solution are easy reduced to the Cu^0 atoms before they are chelated by en and enMe to form Cu-complexes. Therefore, the en and enMe act as not only the

reducing agent but also the chelate ligands, in which the en and enMe as the chelate ligands in the reaction system may partly prevent the reduction from the Cu^{II} cations to Cu^0 atoms due to the chelate effect of en and enMe. Thus the $[Cu(en)_2]^{2+}$ and $[Cu(enMe)_2]^{2+}$ complex cations in the solution are stable and may compensate the charge of the anionic frameworks, which act as not only SDAs for constructing open-frameworks but also framework-forming units for incorporating into the framework.

Structure of 1

Single-crystal X-ray crystallography reveals that **1** crystallizes in the triclinic space group *P*-1. The asymmetric unit consists of two Al atoms, four $B_5O_8(OH)_2$ units, three $[Cu(enMe)_2]^{2+}$ cations and one lattice water molecule (Fig.1). Both Al1 and

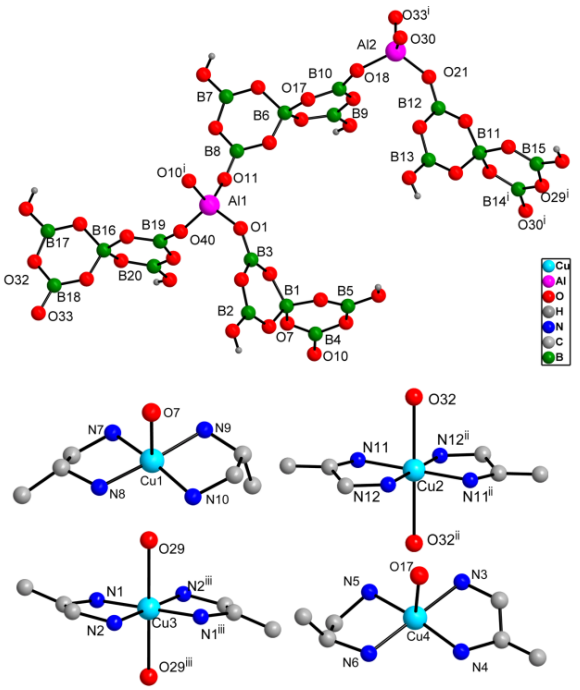

Fig. 1 View of the coordination environments of all Al, B, and Cu atoms in **1**. (Symmetry operation: i) 1+*x*, *y*, *z*; ii) –*x*, 1-*y*, -*z*; iii)-*x*, -*y*, 2-*z*.)

Al2 atoms adopt tetrahedral geometry and the Al-O bond lengths lie between 1.714(4) and 1.750(4) Å (Table S1) and O-Al-O bond angles change from 106.7(2) to 114.5(2)°. In $B_5O_8(OH)_2$ unit, the B atoms reveal three kinds of coordination models for two BO_3 and two $BO_2(OH)$ triangles as well as one BO_4 tetrahedron. The BO_3, $BO_2(OH)$ and BO_4 groups are linked by O atoms to form a pentaborate $[B_5O_8(OH)_2]^{3-}$ cluster, in which two planar B_3O_3 rings are approximatively perpendicular to each other. The B-O band lengths vary froms 1.439(6)-1.509 (7) Å for BO_4 tetrahedra and 1.331(7)-1.404(8) Å for BO_3 triangles. The O-B-O bond angles are distributed in the range of 105.7(4)-112.8(4)° for BO_4 tetrahedra and 114.9(5)-125.1(5)° for BO_3 triangles.

The ABO network of **1** is based on the alternate linkage of AlO_4 groups and $B_5O_8(OH)_2$ clusters. Each AlO_4 group is connected to four others through four bridging $B_5O_8(OH)_2$ clusters, whereas each $B_5O_8(OH)_2$ clusters is connected to six others through two AlO_4 groups (Fig. 2a), forming an unprecedented 4,6-connectivity in ABOs. The common linking mode in layered ABOs is 6-connectivity, in which each AlO_3X group (X = OH, F and so on) is connected to six others by three AlO_3X groups and *vice versa*; while most 3-D ABOs show 11 or 12-connectivity, in which each AlO_4 group is connected to 11 or 12 others by four AlO_4 groups and *vice versa*. It is apparent that in the reported ABOs the AlO_3X groups and oxoboron clusters play an equivalent role in constructing the frameworks. However, the AlO_4 groups and $B_5O_8(OH)_2$ clusters are distinct building units in the construction of **1**. The unique linking mode of 4,6-connectivity leads to a new zigzag layer containing the irregularly shaped 16-membered rings (MRs) delimited by four AlO_4 tetrahedra and four $B_5O_8(OH)_2$ units (Fig. 2b). Therefore, there is no Al-O-Al linking mode in the structure. If the AlO_4 tetrahedra and the $B_5O_8(OH)_2$ clusters are considered as a four-connected node and linkers respectively, the ABO layers can be classified as Shubnikov tetragonal plane (sql) net topology with the total Schläfli symbol of $4^4.6^2$. Although the $B_5O_8(OH)_2$ clusters as linkers has been observed in some chain-like borates [4] and gallium/indium borates,[12] such topology is first reported in ABOs. Interestingly, the Al-Al distances along the *a*-axis have equal lengths of 9.603 (2)Å, while the lengths of two Al-Al distances along the *c*-axis are 9.001(1) and 9.770(2) Å respectively (Fig. 2c).

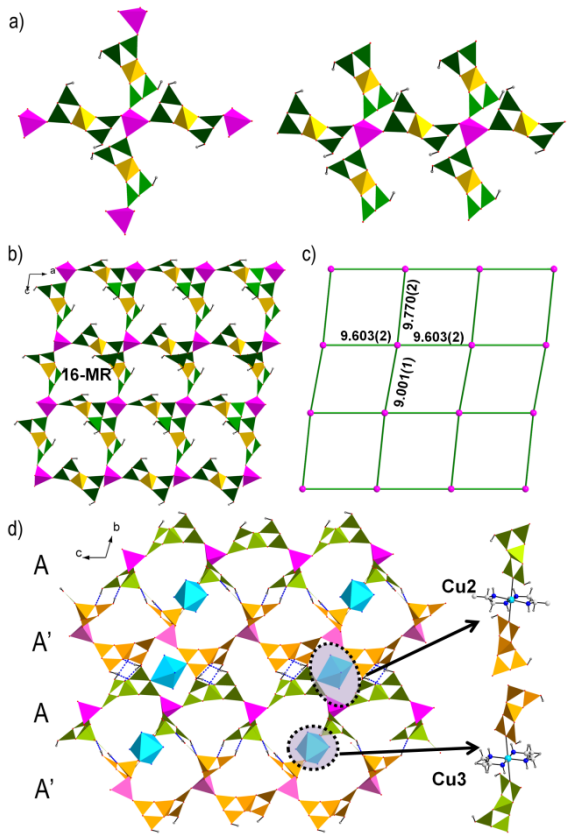

Fig. 2 a) View of the linkage of AlO_4 groups and $B_5O_8(OH)_2$ clusters in **1**. Each AlO_4 unit is bridged by four $B_5O_8(OH)_2$ to four others and each $B_5O_8(OH)_2$ is linked six others via two AlO_4 units. b) View of the ABO layer in **1** made of AlO_4 groups and $B_5O_8(OH)_2$ clusters. Color code: AlO_4, pinkl BO_3, deep green; BO_4, yellow; similarly hereinafter. c) View of the topological network of **1**. d) View of structure **1** along the *bc* plane. Adjacent layers (represented by different colors) are stacked in a sequence -AA'- along the *a*-axis, and further linked by the $[Cu(2,3)(enMe)_2]^{2+}$ complexes to form 3D framework.

The adjacent layers are stacked in an –AA'- sequence along the *b*-axis and linked by O-H···O hydrogen bonds forming a 3-D supramolecular framework containing two types of elliptical 10-MR channels with different sizes between A'-A layers, and peanut shaped 18-MR channels and two opposite 11-MR channels between A-A' layers (Fig. 2d, S2a). The Cu atoms are coordinated by two enMe ligands with the average Cu-N bonds of 2.008(6) Å to form square-planar coordination environment, of which the methyl groups of two enMe coordinated to Cu4 are on the same side and that of other copper atoms are on the opposite sides. The $[Cu2(enMe)_2]^{2+}$ complexes located at the smaller 10-MR channels (Fig. S2c) and the $[Cu3(enMe)_2]^{2+}$ sited in the 18-MR channels (Fig. S2d). Both complexes have two weak axially bound O atoms from borate clusters ($Cu\text{-}O_{av}$ = 2.544 Å) and therefore act as the linkers between adjacent ABO layers. Additionally, the ABO layers are also decorated with the $[Cu1(enMe)_2]^{2+}$ and $[Cu4(enMe)_2]^{2+}$ complexes. Among them, the $[Cu1(enMe)_2]^{2+}$ complexes hung in the ABO layers and the organic part pointed into the 18-MR channels and the larger 10-MR channels (Fig. S2b), whereas $[Cu4(enMe)_2]^{2+}$ complexes located in the 11-MR channels (Fig. S2e). The Cu(1,4) atoms are five coordinated by two enMe and one O atoms, forming a square-pyramid, in which the O atom occupies the axial positions ($Cu\text{-}O_{av}$ = 2.602(4) Å). The weak ligation between unsatured $[Cu(enMe)_2]^{2+}$ complexes and ABO layers is due to the Jahn-Teller effect for d^9 ML_6 octahedral environments. The axial linking mode of Cu-complexes has been successfully used in the linkage of polyoxomolybdate clusters,[13] phosophates[14] as well as germanate clusters.[11a] However, it is the first time that Cu-complexes connect the ABO layers to form 3-D framework, in which the transition metal complexes are the part of the ABO framework.

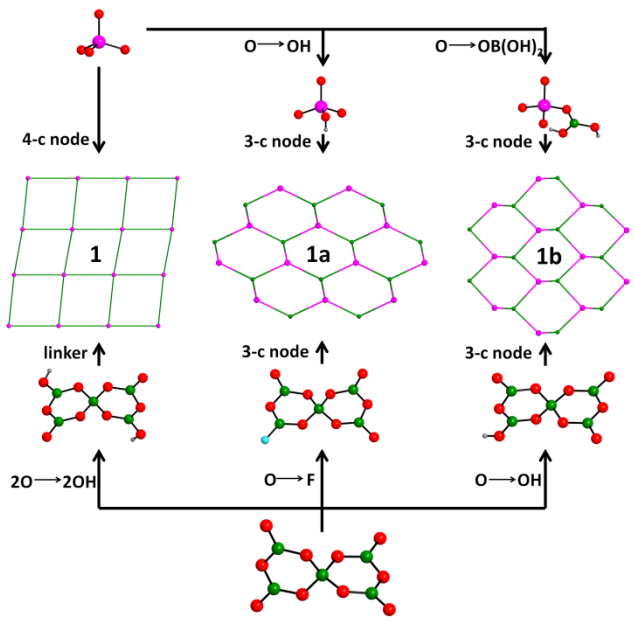

Fig. 3 Comparison of the layer structures in **1**, **1a** and **1b**.

Comparison of the layered ABOs

Microporous layer is often considered as an especial class of porous materials for its unique structural characteristics. However, there are only three examples of ABOs with 2-D layered structures, $[Zn(dien)_2][\{Al(OH)\}\{B_5O_9F\}]$ (**1a**),[8] $[(C_6H_{18}N_2)(AlB_6O_{13}H_3)]$ (**1b**)[15] and $AlB_3O_6(OH)\cdot 0.5(C_2H_{10}N_2)$ (**1c**).[16] Among them, the layer in **1c** is formed by $AlO_3(OH)$ groups and $B_3O_6(OH)$ clusters, while the layers in **1a** and **1b** are constructed from AlO_4 groups and pentaborate clusters. Although **1**, **1a** and **1b** contain similar building unit, it is well worth comparing the three layers (Fig. 3): (1) The pentaborate clusters in **1a** and **1b** can be considered as the B_5O_{10} unit whose one of the four terminal O atoms has been substituted by OH group or F atom and act as three-connected nodes. But in **1**, the pentaborate clusters are regarded as the linkers because two of the terminal O atoms from both sides of the B_5O_{10} cluster are replaced by OH groups and others link to Al atoms. (2) The Al atoms in **1a** and **1b** are bonded to three pentaborate clusters and one terminal OH or $BO(OH)_2$ group, resulting in 3-connected node; while in **1**, the Al atoms are bonded to four borate clusters and act as four-connected nodes. (3) For the different connection mode of Al atoms and pentaborate clusters, the layers in **1a** and **1b** have the common symbol of *hcb* topology, whereas the layers in **1** have *sql* topology. From the viewpoint of structure, it is the substitution of the terminal O atoms of AlO_4 group or B_5O_{10} unit with OH, F or $BO(OH)_2$ groups that prevent the units from further connection.

Structure of 2

Compound **2** crystallizes in the orthorhombic space group *Pbca*. The asymmetric unit of **2** contains one Al atom, one B_5O_{10} unit and one $[Cu(en)_2]^{2+}$ cation (Fig. 4a). The Al atoms are located in general positions and surrounded by four O atoms. All the B atoms are coordinated by three O atoms except the four-coordinated B3 atom. Four BO_3 triangles and one BO_4 tetrahedron are constructed into the B_5O_{10} cluster, in which all the terminal O are further connected. The Al-O and B-O bond lengths ($Al\text{-}O_{av}$ =1.726 (4) Å, $B\text{-}O_{av}$=1.388(6) Å) and O-Al-O and O-B-O bond angles ($O\text{-}Al\text{-}O_{av}$=109.5(2)°, $O\text{-}B\text{-}O_{av}$=116.5(5)°) are in accordance with the reported ABOs.

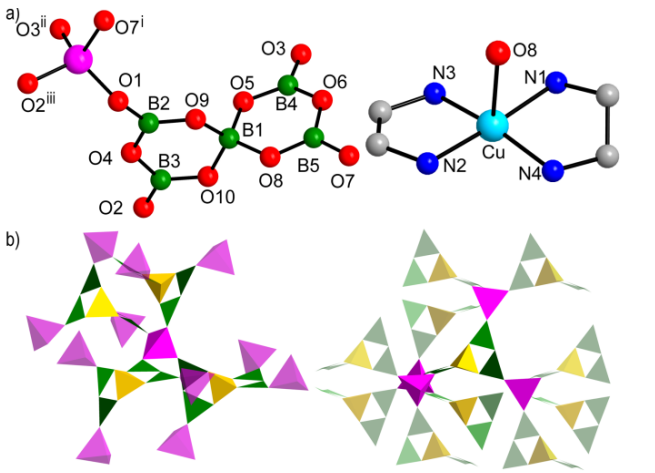

Fig. 4 a) View of the coordination environments of all Al, B, and Cu atoms in **2** (Symmetry operation: i) 0.5+*x*, -0.5-*y*, -1-*z*; ii) 0.5-*x*, -*y*, -1-*z*; iii) 0.5+*x*, *y*, -0.5-*z*.). b) View of the linkage of AlO_4 groups and B_5O_{10} clusters in **2**. Each AlO_4/B_5O_{10} group is bridged by four B_5O_{10}/AlO_4 groups to eleven others.

The overall framework of **2** can be considered as the alternated linkage of AlO_4 groups and B_5O_{10} clusters. Each AlO_4 group links 11 others through four bridging B_5O_{10} clusters, and each B_5O_{10} cluster is also connected to 11 others by four AlO_4 groups (Fig. 4b). From the topological point of view, the frame-

work is a 4-connected uninodal net if each AlO_4 and B_5O_{10} acts as a four-connected node. As a result, **2** has the same topology as $CaGaO_2$ with a total Schläfli symbol of (4.6^5) and the long vertex symbol of $[4{\cdot}6_2{\cdot}6{\cdot}6{\cdot}6{\cdot}6]$ is formed.

The structure consists two types of building layers, of which the idealized layers correspond to the RCSR symbols *hcb* and *fes* in the *bc* and *ab* planes, respectively (Fig. 5). A view along the *a*-axis exposes the *hcb* building layers containing 11-MRs with approximate dimension of 4.45×8.71 $Å^2$ (Fig. S3a). These layers are stacked in a -AA'AA'- sequence, in which the A and A' layers are related by the rotation along the *a*-axis. The 11-MRs in the adjacent layers are disturbed by each other due to the translation. The puckered *fes* layers with 8- and 14-MRs are apparent along the *c*-axis. The oxygen–to–oxygen dimensions of the 8- and 14-MR are about 4.69×6.72 $Å^2$ and 4.66×12.01 $Å^2$, respectively (Fig. S3b). Neighboring layers are related by the translation of 1/2*a*. These layers are packed along the *c*-axis in -BB'- sequence. Interestingly, the *hcb* and *fes* layers exist in parallel to the *ac* plane. It is noteworthy that the shapes and diameters of the 11- and 14-MRs in the two layers are different from those of the layers on the *bc* and *ab* planes: the *hcb* layers on the *ac* plane exhibit more circular-like 11-MRs with the diameter of 5.21×8.79 $Å^2$; the *fes* layers show more circular-like 14-MRs with the diameters of 5.70×11.93 $Å^2$, but the 8-MRs are the same with that on the *ab* plane (Fig. S3c). The two types of building layers are stacked along the *ac* plane in a -AB- sequence. The *hcb* and *fes* building layers resemble those of the reported ABOs[7a,d]. However, the overlapped -AA'-/-BB'- layers have only been observed in rare ABO framework, such as $[CH_3NH_3][(CH_3CH_2)_2NH_2][Al(B_5O_{10})]$.[7a] To the best of our knowledge, it is also first found that different layers are stacked alternately along one direction in ABO structures.

In the structure of **2**, the copper atoms were coordinated by two en ligands (Cu-N = 2.003(5) Å) to form square-planar geometry, which also has a weak axial bond linked to O atoms from the ABO framework (Cu-O = 2.565(4) Å). In other words, the $[Cu(en)_2]^{2+}$ complexes are located at the 11-MRs on the *bc* plane and connected with the framework not only via the weak Cu-O interactions but also with numerous H-bonding interactions from the N atoms of the en to the O atoms of the framework (Fig. S4).

The building layers in 3-D ABO frameworks

It has been observed in zeolite frameworks that different arrangement of building layers can lead to different types of 3-D frameworks. For instance, ZSM-5 and ZSM-11 are both constructed from the same fundamental building layers, and the building layers are connected in different symmetry operations to form ZSM-5 and ZSM-11 different structures.[17] In ZSM-5, the adjacent layers are related by twofold axis, whereas in ZSM-11 the neighboring layers are related by a mirror plane (Fig. S5). Similar examples have also been observed in ABO system. The reported ABO $[CH_3NH_3][(CH_3CH_2)_2NH_2][Al(B_5O_{10})]$ (**2a**), $[CH_3NH_3][CH_3CH_2NH_3](H_2O)_2[Al(B_5O_{10})]$ (**2b**),[7a] QD-3[18] and **2** are both built from the similar building layers with 14- and 8-MRs. Although the rings in the layers are slightly distorted, the compositions and linkage modes of them are just identical. The structure of **2b** and QD-3 (space group $Pna2_1$) are both acentric where the building layers are stacked along *c*-axis or *b*-axis in a sequence of -AAAA- forming the 14- and 8-MR channels. In the centric structure of **2** and **2a** (space group *Pbca*), adjacent building layers are related by the translation and reversion in a -AA'AA'- sequence, and the 14- and 8-MRs are overlapped (Fig. 6).

In order to understand the underlying connection mode of the adjacent layers in **2**, **2a**, **2b** and QD-3, we focus on the 8-MRs in the layers and consider them as quadrangle from the viewpoint of topology. In all of structures, the building layers are constructed in this way that each quadrangle is connected to four neighboring quadrangles. Differently, in **2** and **2a**, each quadrangle further connected to two quadrangles from adjacent layer. In **2b** and QD-3, adjacent layers are interconnected through the linkage of quadrangles one by one to form double zigzag chains. The distinct linkage modes between adjacent layers give rise to two different topological frameworks, namely ABW for **2b** and QD-3 and a new topological type in zeolite for **2** and **2a**. And as the oxoboron clusters are less rigid compared with TO_4 tetrahedra in zeolites, the connections between adjacent building layers are more flexible, which leads to a variety of frameworks and topologies. According to above discussion, it would be a new way to describe the ABO frameworks using the repeated building layers with simple symmetry operations.

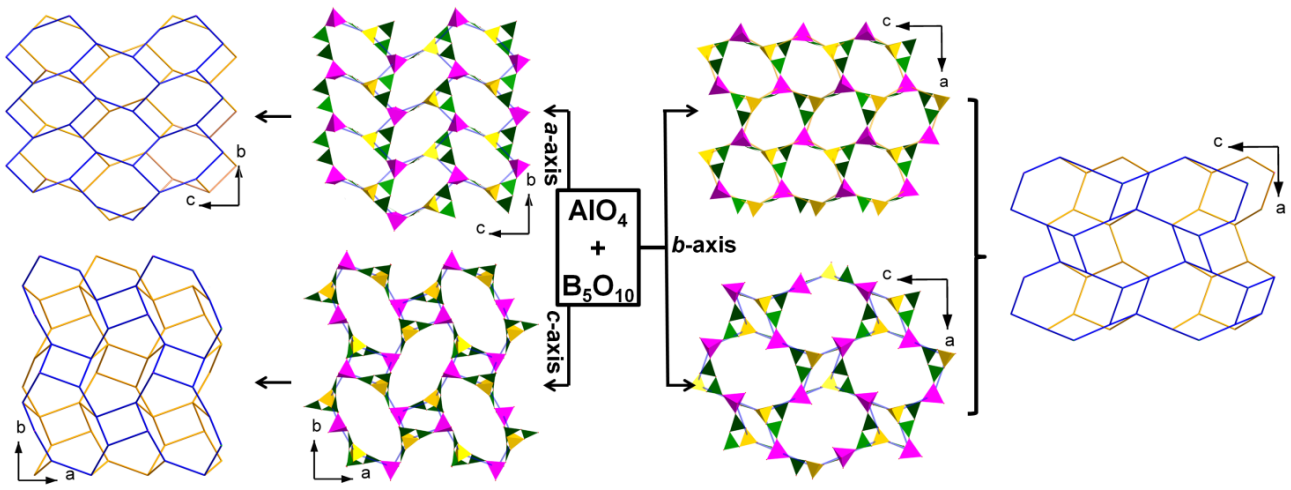

Fig. 5 Polyhedral view of the building layers and the topological view of the stacking of building layers along *a*, *b*, *c*-axis, respectively, in **2**.

Journal Name RSCPublishing

ARTICLE

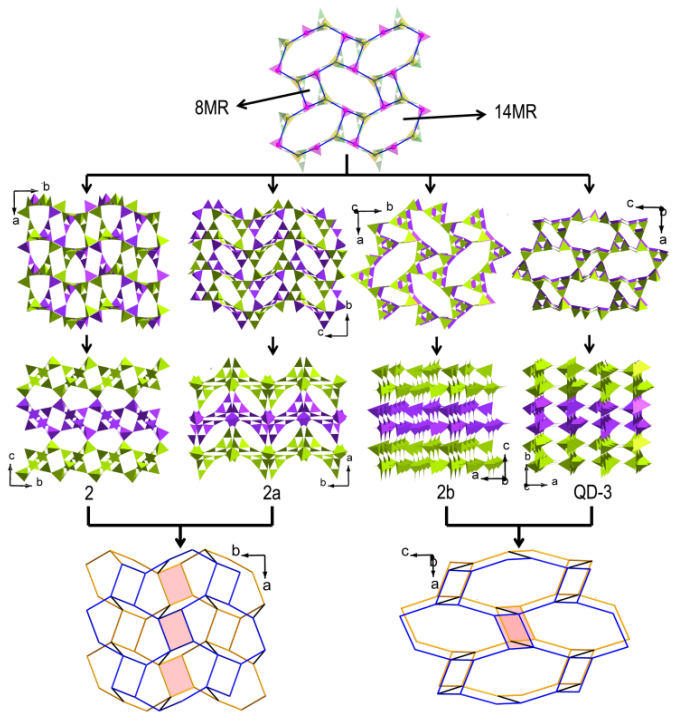

Fig. 6 Comparison of the building layers and the layer stacking in **2**, **2a**, **2b** and QD-3 and the linkage mode of adjacent layers in **2**/**2a** and **2b**/QD-3. (Adjacent layers are described by different colors.)

IR spectroscopy

The broad bands in the IR spectra (Fig. S6) of **1** and **2** at 3440-3250 and 3348-2910 cm^{-1} can be attributed to O-H, N-H and C-H stretching. The asymmetric vibration bands of them can also be observed at 1650-1574 cm^{-1}. The appearance of these resonance signals confirms the presence of amino groups in **1** and **2**. The vibration absorption region of 1460-1400 cm^{-1} is due to B-O asymmetric band stretching of BO_3 and that of BO_4 appears in the range of 1130-1070 cm^{-1}. The bands at 943 cm^{-1} are due to symmetric AlO_4 stretching.

UV-vis-NIR diffuse reflectance spectrum

The UV-vis-NIR diffuse reflectance spectra of **1** and **2** in the region 200-2500 nm are shown in Fig. S7. In their F(R) and E(eV) plots, the band gaps are 3.9 eV for **1** and **2**. The absorption peak centred in 243 nm should be ascribed to the B-O band absorption. The 543 and 573 nm absorption peak is located at green region and yellow-green region, corresponding to the pale red purple crystals of compound **1** and purple crystals of compound **2**, respectively. Both of the absorptions are ascribed to the Cu^{2+} d-d transition.

Thermal behaviour

The TG curve of **1** exhibits two main steps of weight loss (Fig. S8). **1** lost the free water molecules below 200°C with a mass loss of 1.34% close to the theoretical value of 1.15%. Above 200°C, the gradual weight loss of 33.25% up to 700°C was observed and assigned to the removal of the enMe and OH groups (calcd: 32.83%). Compound **2** is stable to 320°C. The TG curve shows two steps of 28.51% in the range from 320 to 700°C, which is in good agreement with the theoretical value of 28.25%, corresponding to the removal of the en molecules.

Conclusion

Two ABOs $[Cu(enMe)_2]_3\{Al_2[B_5O_8(OH)_2]_4\}\cdot H_2O$ (**1**) and $[Cu(en)_2][AlB_5O_{10}]$ (**2**) have been made under solvothermal conditions. **1** contains an ABO layer with irregular 16-MR windows constructed from AlO_4 tetrahedra and $B_5O_8(OH)_2$ clusters. Its ABO layer shows a *sql* net that is different from the known layered ABOs with *hcb* net: in **1**, the AlO_4 group acts as 4-connected node and $B_5O_8(OH)_2$ cluster acts as the linkers, while both AlO_4 group and oxoboron cluster in *hcb* net act as 3-connected nodes. Furthermore, in such a novel linking mode of **1**, each AlO_4 group links four others through four bridging $B_5O_8(OH)_2$ clusters, and each $B_5O_8(OH)_2$ cluster connects six others through two AlO_4 groups. There are two types of copper complexes of $[Cu(2,3)(enMe)_2]^{2+}$ and $[Cu(1,4)(enMe)_2]^{2+}$ in **1**. The former bridges adjacent ABO layers by axial weak Cu-O bonds to form the 3-D framework, the latter only hangs up the interspace of ABO layers. **2** is built up from AlO_4 groups and B_5O_{10} clusters and exhibits *cag* topology. Its framework can be considered as the stacking of the building layers with 8- and 14-MR windows, in which the $[Cu(en)_2]^{2+}$ complexes not only act as the templates but also decorate the pore walls by weak Cu-O bonds. In addition, **2** is the first Cu-complex templated ABOs.

Acknowledgements

This work was supported by the NSFC (Nos. 91122028, 21221001, and 50872133), the 973 Program (Nos. 2014CB932-101 and 2011CB932504), the NSFC for Distinguished Young Scholars (No. 20725101).

Notes and references

1 (a) H. Huang, J. Yao, Z. Lin, X. Wang, R. He, W. Yao, N. Zhai and C. Chen, *Angew. Chem. Int. Ed.*, 2011, **50**, 9141; (b) T. Yang, J. L. Sun, G. B. Li, Y. X. Wang, J. Christensen, Z. B. He, K. E. Christensen, X. D. Zou, F. H. Liao and J. H. Lin, *Inorg. Chem.*, 2009, **48**, 11209; (c) W.-L. Zhang, W.-D. Cheng, H. Zhang, L. Geng, C.-S. Lin and Z.-Z. He, *J. Am. Chem. Soc.*, 2010, **132**, 1508; (d) J. L. C. Rowsell, N. J. Taylor and L. F. Nazar, *J. Am. Chem. Soc.*, 2002, **124**, 6522.

2 P. C. Burns, *Can Mineral*, 1995, **33**, 1167.

3 (a) H. Yu, H. Wu, S. Pan, Y. Wang, Z. Yang and X. Su, *Inorg. Chem.*, 2013, **52**, 5359; (b) X. Dong, H. Wu, Y. Shi, H. Yu, Z. Yang, B. Zhang, Z. Chen, Y. Yang, Z. Huang, S. Pan and Z. Zhou, *Chem.-Eur.*

J., 2013, **19**, 7338; (c) M. S. Wang, G. C. Guo, W. T. Chen, G. Xu, W. W. Zhou, K. J. Wu and J. S. Huang, *Angew. Chem. Int. Ed.*, 2007, **46**, 3909; (d) L. Wang, S. L. Pan, L. X. Chang, J. Y. Hu and H. W. Yu, *Inorg. Chem.*, 2012, **51**, 1852; (e) H. Yu, H. Wu, S. Pan, Z. Yang, X. Su and F. Zhang, *J. Mater. Chem.*, 2012, **22**, 9665.

4 H. X. Zhang, J. Zhang, S. T. Zheng and G. Y. Yang, *Cryst. Growth Des.*, 2005, **5**, 157.

5 (a) Y. F. Li and X. D. Zou, *Angew. Chem. Int. Ed.*, 2005, **44**, 2012; (b) S. Wang, E. V. Alekseev, J. Diwu, W. H. Casey, B. L. Phillips, W. Depmeier and T. E. Albrecht-Schmitt, *Angew. Chem. Int. Ed*., 2010, **49**, 1057; (c) T. Yang, G. Li, L. You, J. Ju, F. Liao and J. Lin, *Chem. Commun.*, 2005, 4225; (d) S. C. Neumair, J. S. Knyrim, O. Oeckler, R. Glaum, R. Kaindl, R. Stalder and H. Huppertz, *Chem.-Eur. J.*, 2010, **16**, 13659.

6 (a) L. M. Meyer and R. C. Haushalter, *Chem. Mater.*, 1994, **6**, 349; (b) L. Allouche, C. Gérardin, T. Loiseau, G. Férey and F. Taulelle, *Angew. Chem. Int. Ed.*, 2000, **39**, 511; (c) K. Wang, J. Yu, P. Miao, Y. Song, J. Li, Z. Shi and R. Xu, *J. Mater. Chem.*, 2001, **11**, 1898.

7 (a) G.-J. Cao, J. Lin, W.-H. Fang, S.-T. Zheng and G.-Y. Yang, *Dalton Trans.*, 2011, **40**, 2940; (b) C. Rong, Z. Yu, Q. Wang, S.-T. Zheng, C.-Y. Pan, F. Deng and G.-Y. Yang, *Inorg. Chem.*, 2009, **48**, 3650; (c) T. Yang, J. Sun, L. Eriksson, G. Li, X. Zou, F. Liao and J. Lin, *Inorg. Chem.*, 2008, **47**, 3228; (d) G.-M. Wang, J.-H. Li, H.-L. Huang, H. Li and J. Zhang, *Inorg. Chem.*, 2008, **47**, 5039; (e) J. Jing, Y. Tao, G. B. Li, F. H. Liao, Y. X. Wang, L. P. You and J. H. Lin, *Chem.-Eur. J.*, 2004, **10**, 3901; (f) J. Ju, J. Lin, G. Li, T. Yang, H. Li, F. Liao, C. K. Loong and L. You, *Angew. Chem. Int. Ed.*, 2003, **42**, 5607; (g) J. Zhou, W. H. Fang, C. Rong and G. Y. Yang, *Chem.-Eur. J.*, 2010, **16**, 4852.

8 J. Zhou, S. T. Zheng, M. Y. Zhang, G. Z. Liu and G. Y. Yang, *CrystEngComm*, 2009, **11**, 2597.

9 P. Kubelka and F. Z. Munk, *Tech. Phys.*, 1931, **12**, 593.

10 (a) G. M. Sheldrick, *SHELXS-97*, Program for Solution of Crystal Structures; University of Göttingen: Germany, 1997. (b) G. M. Sheldrick, *SHELXS-97*, Program for Solution of Crystal Refinement; University of Göttingen: Germany, 1997.

11 (a) C. Cascales, E. Gutiérrez-Puebla, M. Iglesias, M. A. Monge and C. Ruíz-Valero, *Angew. Chem. Int. Ed.*, 1999, 38, 2436; (b) H. H.-Y. Sung, M. M. Wu and I. D. Williams, *Inorg. Chem. Commun.*, 2000, **3**, 401; (c) D. Wragg and R. E. Morris, *J. Mater. Chem.*, 2001, **11**, 513.

12 L. Cheng and G.-Y. Yang, *J. Solid State Chem.*, 2013, **198**, 87.

13 R. P. Bontchev, E. L. Venturini and M. Nyman, *Inorg. Chem.*, 2007, **46**, 4483.

14 P. S. Wheatley and R. E. Morris, *J. Solid State Chem.*, 2002, **167**, 267.

15 A. K. Paul and S. Natarajan, *Cryst. Growth Des.*, 2010, **10**, 765.

16 G. Z. Liu, L. Y. Xin and L. Y. Wang, *Inorg. Chem. Commun.*, 2011, **14**, 775.

17 (a) G. T. Kokotailo, S. L. Lawton, D. H. Olson and W. M. Meier, *Nature*, 1978, **272**, 437; (b) G. T. Kokotailo, P. Chu, S. L. Lawton and W. M. Meier, *Nature*, 1978, **275**, 119.

18 G.-M. Wang, J.-H. Li, Z.-X. Li, H.-L. Huang, S.-Y. Xue and H.-L. Liu, *Inorg. Chem.*, 2008, **47**, 1270.

Table of contents entry

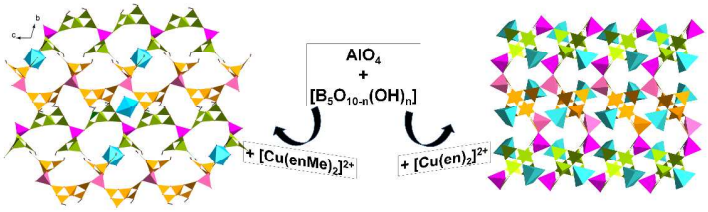

Two novel aluminoborates (**1** and **2**) containing Cu complexes have been made under solvothermal conditions. Both are built from AlO_4 groups and $[B_5O_{10-n}(OH)_n]$ (n = 0 and 2) clusters. **1** features a 2-D aluminoborate layers with 16-member rings, whereas **2** is 3-D framework stacked by different building layers, showing the first Cu-complex directed aluminoborate.